Proceedings of the Korean Nuclear Society Autumn Meeting
Seoul, Korea, October 2001-09-06

PBR_SIM for Depressurization Accident Analysis of Pebble Bed Reactor

Hee Cheon NO
Korea Advanced Institute of Science and Technology

A. C. Kadak
Massachusetts Institute of Technology

Abstract

The PBR_SIM (Pebble Bed Reactor_ SIMulation) code is developed for thermal-hydraulic system dynamic analysis for system control, operational transients, and depressurization accident with/without passive or active concrete cooling system. The primary system including the containment and soil is divided into 12 axial divisions and 20 radial divisions. Radial and axial conduction including radiation, and axial He convection are considered in the core region. In and through the air gap region we consider axial convection and wall convective heat transfer by combination of both air natural convection and forced convection, and radial radiation transport between the reactor vessel and the containment. Radial radiation transport between solid walls is considered through the He gap regions between the core barrel and the inner surface of the reactor vessel, and between the outer surfaces of the reflectors to the inner surface of the reactor vessel. In the containment and soil region only radial conduction heat transfer is considered.

The predictions by PBR_SIM for MPBR at 100% power are compared with those by VSOP. It turns out that the temperature in the upper region in the second channel predicted by PBR_SIM is higher than that by VSOP while that in the lower region is pretty close to each other. The transient capability of PBR_SIM is validated through HEATING-7 analyzing the in stantaneous depressurization accident. The fuel temperature reaches a maximum one of 1679 C at 108 hrs, while the reactor vessel and containment temperatures continue to increase up to 200 hrs.

The effect of the air velocity in the gap region on thermal response during the depressurization accident is investigated. While its effect on the maximum fuel temperature is very small, the maximum reactor vessel and containment temperatures are very significantly affected by the air velocity. For 6m/s, the maximum containment temperature drops below the containment limiting temperature, while the reactor vessel temperature is slightly above the reactor vessel limiting temperature.

1. Model Description

1.1 Description of Primary Thermal-Hydraulic Model

The calculation domain is divided into several major regions: pebble bed region, bottom region, side region and top region. Figure 1 shows the calculation domain including heat transport mechanisms involved in each region.

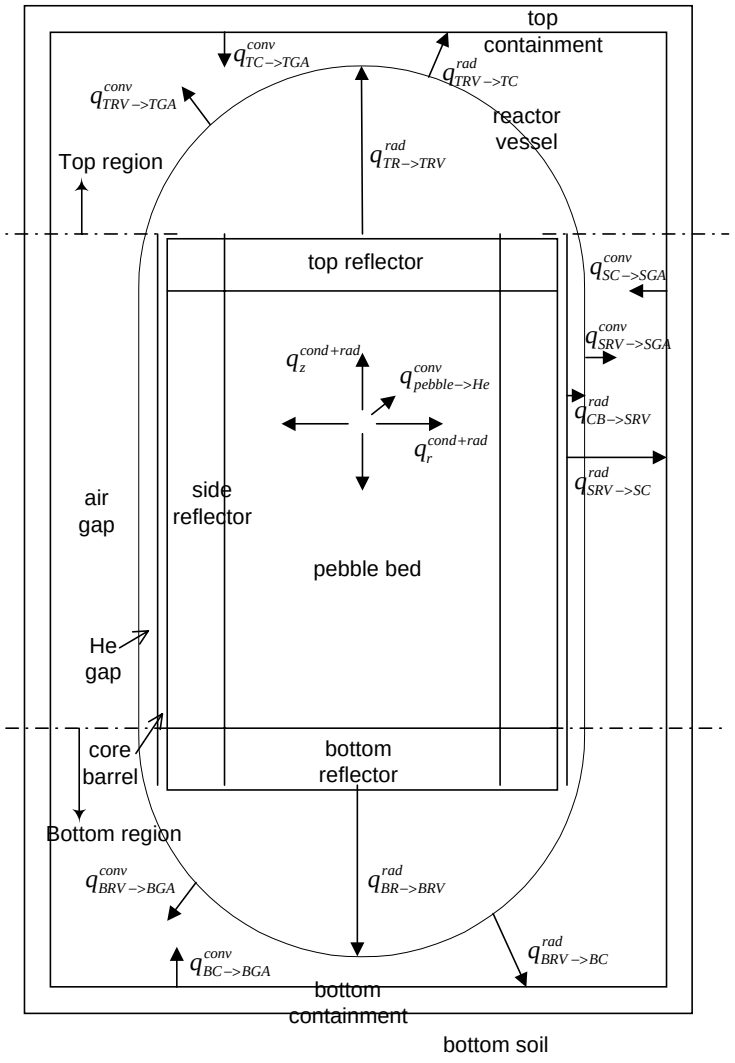

Fig. 1: Calculation domain and heat transport mechanisms involved in each region

(1) Pebble bed region

Let us to use the staggered mesh scheme for the energy conservation equation of the fuel region and the grid scheme for that of the gas coolant as depicted in Fig.2.

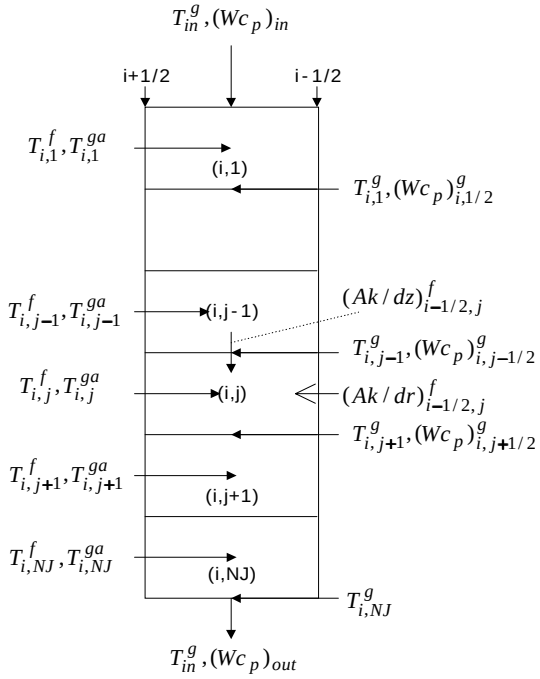

Fig. 2 : Nodal scheme in the pebble bed region

In the staggered mesh scheme and the grid scheme, primary variables calculated by the governing equations are defined at the node and the grid, respectively. In the former interaction between the solid wall and the fluid and the temporary term are better treated, while the primary variables at the outlet are better treated in the latter. Considering the conduction and radiation heat flow in the radial and axial directions and heat exchange between the fuel and coolant gas, we can set up the following governing equation in the pebble bed region:

$$(Mc_p)_{i,j}^{f}\,dT_{i,j}^{f}/dt=(Ak/dr)_{i-1/2,j}^{f}(T_{i-1,j}^{f}-T_{i,j}^{f})+(Ak/dr)_{i+1/2,j}^{f}(T_{i+1,j}^{f}-T_{i,j}^{f})$$
$$+(Ak/dz)_{i,j-1/2}^{f}(T_{i,j-1}^{f}-T_{i,j}^{f})+(Ak/dz)_{i,j+1/2}^{f}(T_{i,j+1}^{f}-T_{i,j}^{f})+(Ah)_{i,j}^{fg}(T_{i,j}^{ga}-T_{i,j}^{f})+q_{i,j}^{'''}V_{i,j}^{f}$$

Neglecting radial energy mixing but considering the axial convection and the heat exchange between the fuel and coolant gas, we use the following governing equation in the gas region:

$$(Mc_p)_{i,j}^{g}\,dT_{i,j}^{g}/dt=(Wc_p)_{i,j-1/2}^{g}T_{i,j-1}^{g}-(Wc_p)_{i,j+1/2}^{g}T_{i,j+1}^{g}+(Ah)_{i,j}^{fg}(T_{i,j}^{f}-T_{i,j}^{ga})$$

where

subscripts i and j: indications of nodes in the r and z directions

superscripts f, g, and fg: indications of fuel and He gas, and interface between fuel and gas

dt, dz, dr: time step size, axial and radial node sizes

k: thermal conductivity including both conduction and radiation

h: convective heat transfer coefficient between fuel and gas

Mc_p : energy capacity in the nodal volume

A and V: surface area and volume

T, W, q''' : temperature, primary mass flow rate of gas, volumetric heat generation

$T_{i,j}^{ga}$: gas temperature in the node (i,j) averaged between the grids, defined as

$$T_{i,j}^{ga} = (T_{i,j-1}^{g} + T_{i,j}^{g}) / 2$$

(2) Reactor vessel, air gap, containment, and soil in the bottom region

To simplify the calculation, it is assumed that heat flux through the bottom containment and soil from the bottom surface of the bottom reflector is the same as that through the side containment and soil from the side surface of the bottom reflector. Here, the bottom region includes reactor vessel, air gap, containment and soil related to the radial path of the heat flux from the side and bottom of the bottom reflector. We estimate the averaged temperature of each radial layer belonging to the bottom region. Based on this simplification, we can set up the following governing equations for each region:

bottom reactor vessel region(BRV)

$$(Mc_p)_{BRV} \frac{dT_{BRV}}{dt} = q_{BR->BRV}^{rad} - (q_{BRV->BGA}^{conv} + q_{BRV->BC1}^{rad})$$

bottom air gap region(BGA)

$$(Mc_P)_{BAG} \frac{dT_{BAG}}{dt} = q_{BRV->BGA}^{conv} + q_{BC1->BGA}^{conv}$$

first node of the bottom containment(BC1)

$$(Mc_p)_{BC1} \frac{dT_{BC1}}{dt} = q_{BRV->BC1}^{rad} - (q_{BC1->BGA}^{conv} + q_{BC1->BC2}^{cond})$$

where

subscripts, BRV, BR, BGA, BC1: indications of bottom reactor vessel, bottom reflector, bottom air gap, and the first node of the containment, and the bottom region is represented by the first axial node except in the bottom air gap in the PBR_SIM

Here, for simplification, the averaged bottom reflector temperature is used to calculate the radiation heat transfer rate:

$$q_{BR->BRV}^{rad} = A_{BR}\varepsilon_{BR}\sigma(T_{BR}^4 - T_{BRV}^4)$$

where

the averaged temperature of the bottom reflector is defined as

$$T_{BR} = \sum_{i=1}^{7} T(i, NJ) / 7 .$$

The governing equations in the second node in the bottom containment and soil is treated using those in the radial direction.

(3) Top reactor vessel, air gap, and containment regions

Heat transfer from the top reflector to the environment above the top containment is dealt with using the following governing equation in each region:

top reactor vessel region(TRV)

$$(Mc_p)_{TRV} \frac{dT_{TRV}}{dt} = q^{rad}_{TR->TRV} - (q^{conv}_{TRV->TAG} + q^{rad}_{TRV->TC})$$

top air gap region(TAG)

$$(Mc_P)_{TAG} \frac{dT_{TAG}}{dt} = q^{conv}_{TRV->TAG} + q^{conv}_{TC->TAG} + W_{air}(T_{air}(NJ) - T_{TAG})$$

top containment(TC)

$$(Mc_p)_{TC} \frac{dT_{TC}}{dt} = q^{rad}_{TRV->TC} - (q^{conv}_{TC->TAG} + q^{cond}_{TC->EA} + q^{rad}_{TC->EST})$$

where

$T_{air}(NJ)$: air temperature in the top grid of the side air gap region,

EST and EA: external structures and external air flow above the top containment, respectively.

In the same way as in the bottom reactor, the averaged top reflector temperature is used to calculate the radiation heat transfer rate:

$$q^{rad}_{TR->TRV} = A_{TR}\varepsilon_{TR}\sigma(T^4_{TR} - T^4_{TRV})$$

where the averaged temperature of the top reflector is defined as

$$T_{TR} = \sum_{i=1}^{7} T(i,1) / 7 .$$

(4) Bottom and top reflector regions

The top reflector region is divided into the same radial nodes as those in the fuel and side reflector regions. The governing equation in each region, (i,1) of the top reflector region is expressed as

$$(Mc_p)_{i,1}\frac{dT_{TR}(i,1)}{dt}=(Ak/dr)^{TR}_{i-1/2,1}(T_{TR}(i-1,1)-T_{TR}(i,1))+(Ak/dr)^{TR}_{i+1/2,1}(T_{TR}(i-1,1)-T_{TR}(i,1))$$
$$+(Ak/dz)^{TR}_{i,3/2}(T_{TR}(i,2)-T_{TR}(i,1))+(Ah)^{rad}_{(i,1)->TRV}(T_{TRV}-T_{TR}(i,1))$$

where

(i,1) and TR denotes the cell index of the top reflector in the r and z directions and the top reflector, respectively.

For radiation heat loss from the top reflector to the top reactor vessel, the region surrounded by both is approximately enclosured and the surface of the i-region in the top reflector is much smaller than that of the top reactor vessel. Then, the radiation heat loss rate is expressed as

$$q^{rad}_{(i,1)->TRV}=(Ah)^{rad}_{(i,1)->TRV}(T_{TRV}-T_{TR}(i,1))=A(i,1)\sigma\varepsilon_{TR}(T^4_{TR}-T^4_{TRV}(i,1))$$

Also, the coefficients of the conductive heat transfer rates is expressed as

$$(Ak/dr)^{TR}_{i-1/2}=A^r_{i-1/2,1}/\left[dr(i-1)/(2k_{i-1,1})+dr(i)/(2k_{i,1})\right]$$

$$(Ak/dz)^{TR}_{i,2/3}=A^z_{i-1/2,1}/\left[dz(1)/(2k_{i,1})+dz(2)/(2k_{i,2})\right]$$

The bottom reflector region is treated in the similar way to the top reflector region. The governing equation in each radial node, (i,NJ) of the bottom reflector region:

$$(Mc_p)_{i,NJ}\frac{dT_{BR}(i,NJ)}{dt}=(Ak/dr)^{BR}_{i-1/2,NJ}(T_{BR}(i-1,NJ)-T_{BR}(i,NJ))+(Ak/dr)^{BR}_{i+1/2,NJ}*$$
$$(T_{BR}(i+1,NJ)-T_{BR}(i,NJ))+(Ak/dz)^{BR}_{i,NJ-1/2}(T_{BR}(i,NJ-1)-T_{BR}(i,NJ))+(Ah)^{rad}_{(i,NJ)->BRV}(T_{BRV}-T_{BR}(i,NJ))$$

where NJ, BR,BRV denote the axial index of the bottom reflector region, and indication of the bottom reflector and bottom reactor vessel, respectively.

(5) Side reactor vessel region

As the thickness of the side reactor vessel is thin enough compared with its length, only heat transfer in the radial direction is dominant over that in the axial direction:

$$(Mc_p)_{SRV}\frac{dT_{SRV}(i,j)}{dt}=q^{rad}_{CB->SRV}-(q^{conv}_{SRV->SGA}+q^{rad}_{SRV->SC})$$

where

$q^{rad}_{CB->SRV}, q^{rad}_{SRV->SC}, q^{conv}_{SRV->SGA}$ denote radiation heat transfer rates from the core barrel to the side reactor vessel, and from the side reactor vessel to the side containment, and the convective heat transfer from the side reactor vessel to the side air gap, respectively.

(6) Core barrel region

As the thickness of the core barrel is thin enough compared with its length, only heat transfer in the radial direction is dominant over that in the axial direction:

$$(Mc_p)_{CB}\frac{dT_{CB}(i,j)}{dt} = q^{cond}_{SR->CB} - q^{rad}_{CB->SRV}$$

where

$q^{cond}_{SR->CB}, q^{rad}_{CB->SRV}$: conductive heat transfer rate from the side reflector to the core barrel and radiation heat transfer rate from the core barrel to the side reactor vessel defined as

$$q^{rad}_{CB->SRV} = \sigma(T^4_{CB} - T^4_{SRV}) / \left[\varepsilon_{CB}/(\varepsilon_{CB}A_{CB}) + (1-\varepsilon_{SRV})/(\varepsilon_{SRV}A_{SRV})\right]$$

$$q^{cond}_{SR->CB} = (Ak/dr)_{i-1/2,j}(T_{SR}(i-1,j) - T_{CB}(i,j))$$

(7) Side containment and soil region

As the thermal gradient in the radial direction is much higher than that in the axial direction, only heat transfer in the radial direction is considered:

first node of the side containment

$$(Mc_p)_{SC}\frac{dT_{SC}(i,j)}{dt} = q^{rad}_{SRV->SC} - q^{conv}_{SC->SGA} - q^{cond}_{SC}$$

The three terms in the left-handed side represent the heat transfer rate by radiation from the side reactor vessel to the side containment, convection from the side containment to the side gap air, and conduction from the first node of the containment to the second node of the containment, defined as

$$q^{rad}_{SRC->SC} = \sigma(T^4_{SRV}(i-2,j) - T^4_{SC}(i,j)) / \left[\varepsilon_{SRV}/(\varepsilon_{SRV}A_{SRV}) + (1-\varepsilon_{SC})/(\varepsilon_{SC}A_{SC})\right]$$
$$q^{conv}_{SC->SGA} = A_{SC}(i,j)h^{conv}_{SC->SGA}(T_{SC}(i,j) - T_{SGA}(i-1,j))$$
$$q^{cond}_{SC} = (Ak/dr)_{i+1/2.j}(T_{SC}(i,j) - T_{SC}(i+1,j))$$

general relationship in the remaining nodes of the side containment and soil

$$(Mc_p)_{i,j}\frac{dT_{SC}(i,j)}{dt} = q^{cond}_{i-1/2,j} - q^{cond}_{i+1/2,j}$$

where

$$q^{cond}_{i-1/2,\,j} = (Ak/dr)_{i-1/2,\,j}\,(T(i-1,\,j) - T(i,\,j))$$

(8) Air gap region

Let us use the grid scheme for the energy equation of the air gap region shown in Fig.3.

The air in the air gap flows from its bottom to its top. Then, the governing equation is expressed as

$$(Mc_p)^g_{i,j}\,dT^g_{i,j}/dt = (Wc_p)^g_{i,j'-1/2}\,T^g_{i,j-1} - (Wc_p)^g_{i,j'+1/2}\,T^g_{i,j+1} +$$
$$(Ah)^{rg}_{i,j'}\,(T^f_{i-1,j'} - T^{ga}_{i,j}) + (Ah)^{cg}_{i,j'}\,(T^f_{i+1,j'} - T^{ga}_{i,j})$$

where

the superscripts, g,rg,cg represent the air, heat transfer from the reactor to the air and from the containment to the air.

The subscripts, i,i-1,i+1 represent the index of the air, the reactor vessel, and the containment, and j' the same axial plane counted from the top because the axial index, j, in the reactor and the containment is counted from the top and the bottom, defined as

$$j' = NJ - j + 1\,.$$

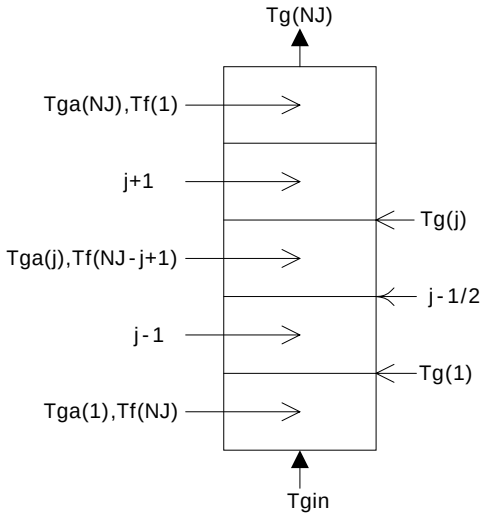

Fig. 3 : Grid scheme in the air gap region

1.2 Description of Core Neutronics Models

The point reactor kinetics equations for the one effective group of delayed neutrons becomes

$$dQ/dt = (\rho - \beta)Q/\Lambda + \lambda C$$
$$dC/dt = \beta Q/\Lambda - \lambda C$$

where

β, ρ, Λ : total yield fraction, reactivity, mean neutron generation speed

Q, C : total reactor thermal power, precursor concentration

The rate equations for Xenon and Iodine are given by

$$dI/dt = \gamma_I \Sigma_f \phi - \lambda_I I$$
$$dXe/dt = \gamma_{Xe} \Sigma_f \phi + \lambda_I I - (\lambda_{Xe} + \sigma_a^{Xe} \phi) Xe$$

The reactivity from Xe concentration is estimated by

$$\Delta\rho = -\sigma_a^{Xe} Xe / \Sigma_a$$

The temperature coefficients of reactivity is estimated using the data of the MGR-GT reactor(1).

Considering the dependence of decay heat production on reactor power level prior to shutdown, the history of the operation, and the shutdown period of time, the following KFA formula(1) is used to approximate the decay heat generation:

$$Q_{decay}/Q_0 = A((t_s^{-a} - (t_0 + t_s)^{-a})$$

1.3 Solution Scheme

The solution scheme is based on the explicit time scheme:

$$dy/dt = f(x) -> y^{n+1} = y^n + f(x^n)dt$$

Let us take the example of the governing equations in the fuel region to explain the numerical scheme. The energy equations for the fuel and coolant gas in the pebble bed region are converted into the following numerical equations:

$$(Mc_p)_{i,j}^f (T_{i,j}^{f,n+1} - T_{i,j}^{f,n})/\Delta t = (Ak/dr)_{i-1/2,j}^f (T_{i-1,j}^{f,n} - T_{i,j}^{f,n}) + (Ak/dr)_{i+1/2,j}^f (T_{i+1,j}^{f,n} - T_{i,j}^{f,n})$$
$$+ (Ak/dz)_{i,j-1/2}^f (T_{i,j-1}^{f,n} - T_{i,j}^{f,n}) + (Ak/dz)_{i,j+1/2}^f (T_{i,j+1}^{f,n} - T_{i,j}^{f,n}) + (Ah)_{i,j}^{fg} (T_{i,j}^{g,n} - T_{i,j}^{f,n}) + q_{i,j}''' V_{i,j}^f$$

$$(Mc_p)_{i,j}^g (T_{i,j}^{g,n+1} - T_{i,j}^{g,n})/\Delta t = (Wc_p)_{i,j-1/2}^g T_{i,j-1}^{g,n} - (Wc_p)_{i,j+1/2}^g T_{i,j+1}^{g,n} + (Ah)_{i,j}^{fg} (T_{i,j}^{f,n} - T_{i,j}^{g,n})$$

The above equations are expressed in terms of time constants:

$$(T_{i,j}^{f,n+1} - T_{i,j}^{f,n})/\Delta t = (1/\tau_{i-1/2,j}^{f,n})(T_{i-1,j}^{f,n} - T_{i,j}^{f,n}) + (1/\tau_{i+1/2,j}^{f,n})(T_{i+1,j}^{f,n} - T_{i,j}^{f,n})$$
$$+ (1/\tau_{i,j-1/2}^{f,n})(T_{i,j-1}^{f,n} - T_{i,j}^{f,n}) + (1/\tau_{i,j+1/2}^{f,n})(T_{i,j+1}^{f,n} - T_{i,j}^{f,n}) + (1/\tau_{i,j}^{fg,n})(T_{i,j}^{g,n} - T_{i,j}^{f,n}) + q_{i,j}^{f,n}$$

$$(T_{i,j}^{g,n+1} - T_{i,j}^{g,n})/\Delta t = (1/\tau_{i,j-1/2}^{g,n})T_{i,j-1}^{g,n} - (1/\tau_{i,j+1/2}^{g,n})T_{i,j+1}^{g,n} + (1/\tau_{i,j}^{fg,n})(T_{i,j}^{f,n} - T_{i,j}^{g,n})$$

where the various time constants are defined as

$$\tau_{i-1/2,j}^{f,n} = (Mc_p)_{i,j}^{f} / (Ak/dr)_{i-1/2,j}^{f}$$
$$\tau_{i+1/2,j}^{f,n} = (Mc_p)_{i,j}^{f} / (Ak/dr)_{i+1/2,j}^{f}$$
$$\tau_{i,j-1/2}^{f,n} = (Mc_p)_{i,j}^{f} / (Ak/dz)_{i,j-1/2}^{f}$$
$$\tau_{i,j+1/2}^{f,n} = (Mc_p)_{i,j}^{f} / (Ak/dz)_{i,j+1/2}^{f}$$
$$\tau_{i,j}^{f,n} = (Mc_p)_{i,j}^{f} / (Ah)_{i,j}^{fg}$$
$$q_{i,j}^{f,n} = q_{i,j}^{'''} V_{i,j}^{f} / (Mc_p)_{i,j}^{f}$$

$$\tau_{i,j-1/2}^{g,n} = (Mc_p)_{i,j}^{g} / (Wc_p)_{i,j-1/2}^{g}$$
$$\tau_{i,j+1/2}^{g,n} = (Mc_p)_{i,j}^{g} / (Wc_p)_{i,j+1/2}^{g}$$
$$\tau_{i,j}^{fg,n} = (Mc_p)_{i,j}^{g} / (Ah)_{i,j}^{fg}$$

As the explicit numerical scheme is used, the time step size should be limited by two conditions, convective limit and conductive limit to maintain numerical stability, defined as

Courant limiting condition: $\Delta t < \min(\Delta z / v_{axial}^{g}, \Delta z / v_{axial}^{a})$

Conduction limiting condition: $\Delta t_{CondL} < \min(\Delta r^2/\alpha, \Delta z^2/\alpha)$

1.4 Physical models

(1) Pebble bed region

Pebble bed effective thermal conductivity

For Pebble bed effective thermal conductivity, k(T), the following simplified correlation developed by General Electric(3) is used:

$$k(T) = 1.1536x10^{-4}(T - 173.16)^{1.6632}$$

where k(T): temperature dependent thermal conductivity of pebble bed, W/m-k

Convective heat transfer coefficient between fuel and gas

The following heat transfer correlations are used to calculate the heat transfer from the fuel and to the gas: Here, the heat transfer coefficient, h, for forced convection is calculated based on the correlation developed by KFK(2):

$$h = (k/d)Nu$$

where

$$Nu = 1.27\,\mathrm{Pr}_g^{0.333}\,\mathrm{Re}_g^{0.36}/\varepsilon^{1.18} + 0.033\,\mathrm{Pr}_g^{0.5}\,\mathrm{Re}_g^{0.86}/\varepsilon^{1.07}$$

where

$$Q_{i,j}^{fg} = (Ah)_{i,j}^{fg}(T_{i,j}^{f} - T_{i,j}^{g})$$
$$\mathrm{Re}_g = (W_g d_{ball})/(A_c \mu_g)$$

d_{ball} : diameter of the ball(m)

A_c and A^{fg} : empty-core cross section area and total surface ball area

ε: porosity estimated using the following empirical relationship (4):

$$\varepsilon = 0.78/(D_{bed}/d_{ball})^2 + 0.375$$

(2) Radiation heat transfer

Radiation heat transfer through the gas gap is estimated using the following basic radioactive heat transfer equation (5):

$$Q_{Rij,i+1j} = A_{i,j}\sigma\varepsilon_{ij,i+1j}(T_{i,j}^4 - T_{i+1,j}^4) = A_{i,j}h_{ij,i+1j}(T_{i,j} - T_{i+1,j})$$

where

$Q_{Rij,i+1j}$: radioactive heat transfer rate between nodes, (i,j) and (i+1,j)

h: effective heat transfer coefficient between nodes, (i,j) and (i+1,j) defined as

$$h_{Rij,i+1j} = \sigma\varepsilon_{ij,i+1j}(T_{i,j}^2 + T_{i+1,j}^2)(T_{i,j} + T_{i+1,j})$$

Emittance from nodes (i,j) and (i+1,j) is defined as

$$\varepsilon_{ij,i+1j} = 1/\left[(1-\varepsilon_{i+1,j})/(\varepsilon_{i+1,j}A_{i+1,j}) + 1/(A_{ij}F_{ij,i+1j}) + (1-\varepsilon_{i,j})/(\varepsilon_{i,j}A_{i,j})\right]$$

where

$F_{ij,i+1j}$: view factor between two planes, (i,j) and (i+1,j)

(3) Convective heat transfer coefficient by air in the air gap

$$h_g = k_g Nu_g / dr_g$$

where

$$Nu_g = (Nu_f + Nu_n)^{1/3}$$
$$Nu_{fg} = 0.023 \mathrm{Re}_g^{0.8} \mathrm{Pr}_g^{1/3}$$
$$Nu_n = C_n \left[(T_w - T_g)/(T_w + T_g) \right]^{1/3}$$

The Nusselt number for natural circulation flow, Nu_n, is obtained using the well-known correlations for the horizontal and vertical plates(6) defined as:

$C_n = 0.15 \left[2gc_p \rho_g^2 / (k_g \mu_g) \right]^{1/3}$ for the horizontal plate

$= 0.1 \left[2gc_p \rho_g^2 / (k_g \mu_g) \right]^{1/3}$ for the vertical plate

The properties for the convective heat transfer coefficients are estimated at the averaged temperature of the gas and the wall.

The total Nusselt number for gas flow, Nu_g, is combined by two contributions, forced convective, Nu_f, and natural convective, Nu_n:

$$Nu_g = (Nu_f^3 + Nu_n^3)^{1/3}$$

2. Simulation and Validation of PBR_SIM

For the simulation of PBR_SIM the actual geometry of the pebble bed region of MPBR is approximated into the cylinders of 5 channels with the ten axial divisions with the initial and boundary conditions of Table 1.

At 100% power MPBR is simulated using the following power distribution at equilibrium fuel cycle

HEATING-7(Heat Engineering and Transfer In Nine Geometries-7)(10) is a multidimensional, general-purpose heat transfer code written in FORTRAN 77. HEATING solves steady-state and/or transient problems in one-, two-, or three-dimensional Cartesian, cylindrical, or spherical coordinates. The code can deal with the conduction and radiation problem only. However, it can not deal with any convective problem. Therefore, in case of no air flow in the air gap region, predictions by PBR_SIM are compared with those by HEATING-7 for the V&V of PBR_SIM. After then, the effect of air velocities on thermal response of MPBR is investigated.

Table1: boundary and initial conditions simulated in PBR_SIM

parameters	initial conditions
total core power	265 Mw(th)
total core flow rate	118.87 kg/s
primary pressure	8 MPa
He coolant inlet temperature	445 C
pressure vessel temperature	280 C
external air and structures	35 C
concrete	50 C
earth	35 C
parameters	boundary conditions
external air and structures	35 C
outer most boundary of earth	35 C

The predictions by PBR_SIM for MPBR at 100% power are compared with those by VSOP(Very Superior Old Program) for computer code system for reactor physics and fuel cycle simulation. The input for VSOP is produced for PBMR of ESKOM. The inlet and outlet temperatures are 536C and 900C. Two cases are compared as shown in Figs. 4 and 5: axial temperature distribution in the second channel and the radial distribution in the axial plane of 6.53m from the top of the pebble bed region. It turns out that the temperature in the upper region in the second channel predicted by PBR_SIM is higher than that by VSOP while that in the lower region is pretty close to each other. The lower predictions by PBR_SIM may be caused by absence of He region between the top reflector and the top of the pebble bed region in PBR_SIM. In the same way, the temperature in the center reflector predicted by PBR_SIM is lower than that by VSOP.

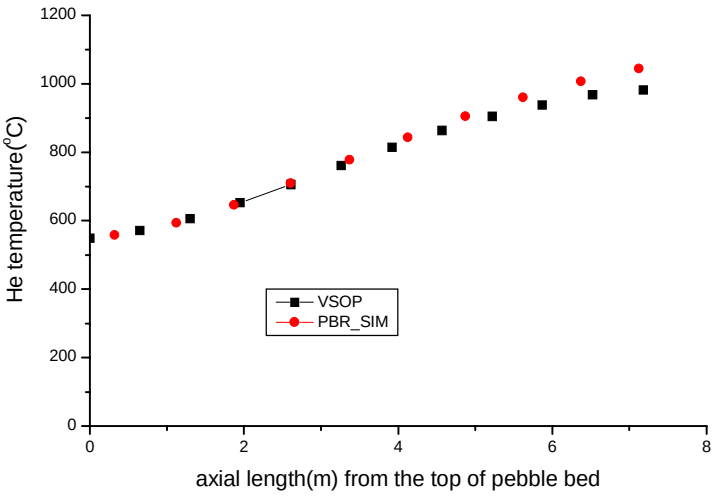

Fig. 4 : Axial temperature distribution in the 3rd channel at 100% power

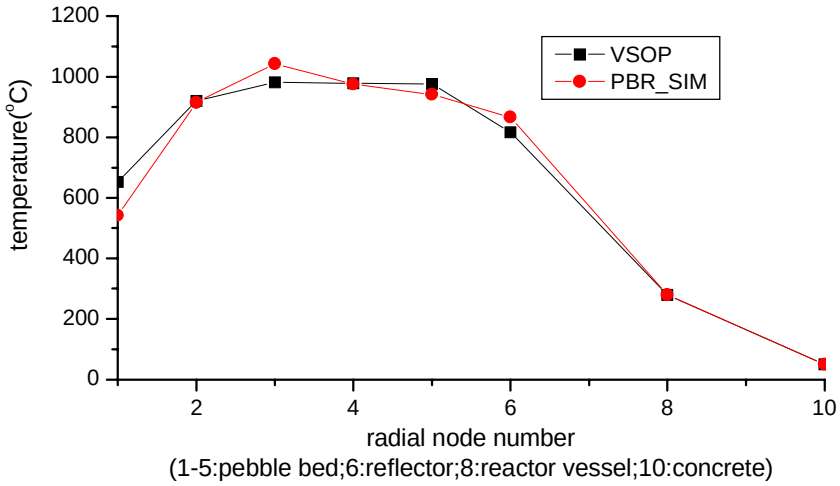

Fig. 5 : Radial temperature distribution in the axial plane of 7.125m from top at 100% power

The instantaneous depressurization accident, in which shutdown and complete depressurization at the start of transient take place, is simulated using PBR_SIM and HEATING-7. The operational requirements of MPBR are as follows:

According the DOE report performed by Bechtel, the concrete temperatures should be less than 65 C during normal operation and 177 C for off-normal transients and the reactor vessel temperatures should be less than 427 C during normal operation and 482 C for off-normal transients. As shown in figure, the fuel temperature reaches a maximum one of 1679 C at 108 hrs the 7^{th} node in the second channel from the top of the core region when the heat loss from the reactor vessel is higher than heat generation in the pebble bed region. However, the reactor vessel and containment temperatures continue to increase up to 200 hrs. Figure 6 shows comparison of predictions by PBR_SIM and those by HEATING-7. There is in good agreement among them.

The effect of the air velocity in the gap region on thermal response during the depressurization accident is investigated. As shown in Fig.7, while its effect on the maximum fuel temperature is very small, the maximum reactor vessel and containment temperatures are very significantly affected by the air velocity. For 2m/s of the air velocity, the peak temperatures and times of the fuel, reactor vessel, containment are reached at 1663 C and 89 hr, 593 C and 47 hr, and 305 C and 128 hr, respectively. For 6m/s, the maximum containment temperature drops below the containment limiting temperature, while the reactor vessel temperature is still above the reactor vessel limiting temperature. In order to protect the reactor vessel, we need to install the thermal shield with lower thermal conductivity such as carbon material than graphite between the side reflector and the reactor vessel.

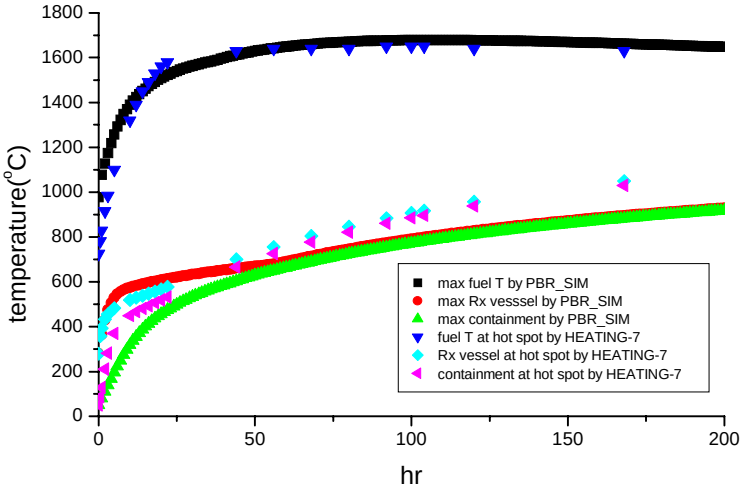

Fig. 6 : Comparison of predictions by PBR_SIM with those by HEATING-7

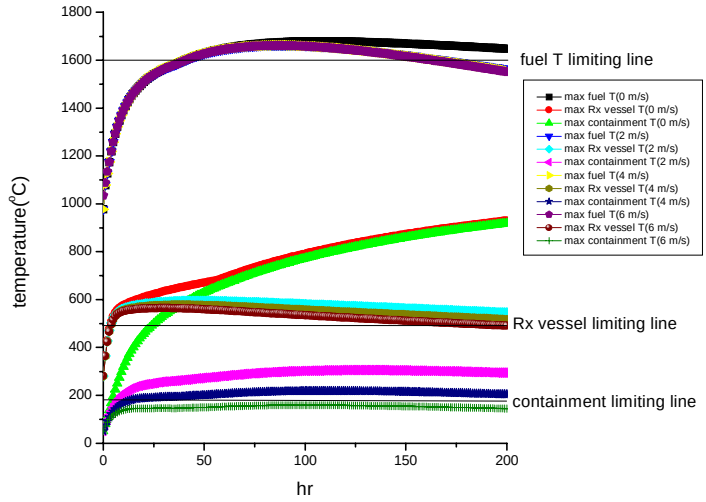

Fig. 7 : Trends of maximum temperature for 0.2, 4.6 m/s of air velocity in the air gap region

3. Conclusions

The PBR_SIM code is developed for thermal-hydraulic system dynamic analysis for depressurization accident with/without passive or active concrete cooling system.

Through VSOP the steady-state capability of PBR_SIM is validated. It turns out that the temperature in the upper region in the second channel predicted by PBR_SIM is higher than that by VSOP while that in the lower region is pretty close to each other. Also, the transient capability of PBR_SIM is validated through HEATING-7 analyzing the instantaneous depressurization accident. The effect of the air velocity in the gap region on thermal response during the depressurization accident is investigated. While its effect on the maximum fuel temperature is very small, the maximum reactor vessel and containment temperatures

are very significantly affected by the air velocity. For 6m/s, the maximum containment temperature drops below the containment limiting temperature, while the reactor vessel temperature is slightly above the reactor vessel limiting temperature.

References

1) X. Yan, 'Dynamic Analysis and Control System Design for an Advanced Nuclear Gas turbine Power Plant,' M.I.T., Ph.D. Thesis (1990)

2) Saphier, D,"HTGR Transient Analysis with the DSNP Simulation Language," RASG-111-84, Soreg Nuclear Research Centew, Israel, (1984)

3) "Warmeubergang im Kugelhaufen," KTA 3102, (1978)

4) Edited by Henri Fenech, 'Heat Transfer and Fluid Flow in Nuclear System', Pergamon Press

5) F. P. Incropera and D. P. De Witt, 'Fundamentals of heat and Mass Transfer,' John Wiley & Sons, Inc, (1990)

6) M. G. Savage, "A one-dimensional Modeling of Radial Heat Removal During Depressurized Heatup transients in Modular Pebble-bed and Prismatic High Temperature Gas-cooled Reactors," ORNL/TM-9215, Oak Ridge National Laboratory (1984)

7) R.E. Nightingale, ed., 'Nuclear Graphite,' Academic Press (1962)

8) G.J. van Tuyle, T.C. Nepsee, and J.G. Guppy, "MINET Code Documentation," BNL-NUREG-51742, BNL (1984)

9) S. Yang, 'Heat Transfer,' (1987)

10) Computing Applications Division of Oak Ridge National Laboratory. "Manual for HEATING-7 (Multidimensional, Finite-Difference Heat Conduction Analysis Code System) Version 7.2I and 7.3" (1997)

11) E. Teuchert, et. al., 'VSOP: Input Manual and Comments' Forschungszentrum Julich GmbH, Jul-2897, (1994)

12) Bechtel National, INC., 'HFD-35600: Reactor Cavity Cooling System Design Description,' DOE-HTGR-87-068 (1987)